Insights into the farming-season carbon budget of coastal earthen aquaculture ponds in southeastern China

Ping Yang[a,b,c,*], Kam W. Tang[d], Hong Yang[e], Chuan Tong[a,b,c,*], Nan Yang[a], Derrick Y. F. Lai[f], Yan Hong[a], Manjing Ruan[a], Yingying Tan[a], Guanghui Zhao[a], Ling Li[a], Chen Tang[a]

[a]*School of Geographical Sciences, Fujian Normal University, Fuzhou 350007, P.R. China,*

[b]*Key Laboratory of Humid Subtropical Eco-geographical Process of Ministry of Education, Fujian Normal University, Fuzhou 350007, P.R. China,*

[c]*Research Centre of Wetlands in Subtropical Region, Fujian Normal University, Fuzhou 350007, P.R. China,*

[d]*Department of Biosciences, Swansea University, Swansea SA2 8PP, U. K.*

[e]*Department of Geography and Environmental Science, University of Reading, Reading, RG6 6AB, UK*

[f]*Department of Geography and Resource Management, The Chinese University of Hong Kong, Hong Kong, China*

***Correspondence to:**

Ping Yang (yangping528@sina.cn), Chuan Tong (tongch@fjnu.edu.cn)

Telephone: 086-0591-87445659 Fax: 086-0591-83465397

A B S T R A C T

Small-hold aquaculture ponds are widespread in China, but their carbon greenhouse gas emissions are poorly quantified. In this study, we used a carbon budget approach to assess the climate footprint of three earthen aquaculture ponds in southeastern China with the whiteleg shrimp (*Litopenaeus vannamei*) during the farming period. The main carbon inputs to the ponds were planktonic primary production (58.5–61.8%), followed by commercial feeds (31.9-35.3%), while the major carbon outputs occurred through planktonic respiration (44.0–53.6%) and sedimentation (18.0–21.7%). Water-to-air emissions of carbon greenhouse gases (CO_2 and CH_4) represented only a small fraction of the carbon flow (0.8–1.6%), with a combined CO_2-equivalent emission of 528.4±193.3 mg CO_2-eq m^{-2} h^{-1} based on GWP_{20}. We also observed significant spatio-temporal variation in carbon greenhouse gases among the three ponds, which could be attributed to the variation in Chl-*a* and carbon substrate supply. Nevertheless, the magnitude of CH_4 emission from these ponds was still higher than some other agro-ecosystems. Moreover, we found that only 21% of the excess organic carbon was converted to shrimp biomass, while another 20% ended up in the sediment. Our findings suggested that lowering the feed conversion ratio and removing the bottom sediments regularly could help improve production efficiency, reduce the excessive accumulation of carbon-rich detritus and minimize the climatic warming impacts of aquaculture production.

Keywords: Aquaculture ponds; Carbon budget; Carbon dioxide; Methane; Global warming potential

List of abbreviations:

***A*P:** Atmospheric Pressure

CH_4: Methane

Chl-*a*: Chlorophyll *a*

CO_2: Carbon dioxide

DO: Dissolved Oxygen

DOC: Dissolved Organic Carbon

GCE: Gaseous carbon (CO_2 and CH_4) emission

GWP_{20}: Global Warming Potential (20-year time horizon)

HA: Harvested Animals

IW: Inflow Water

OW: Outflow Water

PP: Primary Production

PR: Water-column respiration

POC: Particulate Organic Carbon

SA: Sediment Accumulation

SR: Sediment Respiration

SOD: Sediment Oxygen Demand

T_A: Air Temperature

TC: Total Carbon

T_W: Water Temperature

W_S: Wind Speed

1. Introduction

Since the Industrial Revolution, the atmospheric concentrations of the two main greenhouse gases (GHGs), carbon dioxide (CO_2) and methane (CH_4), have increased respectively by about 44% and 156% since 1750, reaching 419 ppm and 1.909 ppm, respectively, in 2022 (NOAA, 2022). Aquatic habitats are important sources of global CO_2 and CH_4 emissions (Bastviken et al., 2011; Li et al., 2018; Tranvik et al., 2009; Yang et al., 2011); therefore, understanding the carbon greenhouse gas dynamics in these habitats will help mitigate global warming and the related impact on ecosystem (Yang et al., 2020).

Increasing global food demand has led to the rapid expansion of aquaculture world-wide, especially small-hold aquaculture ponds (FAO, 2018; Ren et al., 2019), raising concerns about their environmental impacts including GHG emissions (Datta et al., 2009; Frei et al., 2007; Yuan et al., 2019). Despite their small size, small-hold aquaculture ponds can have high water-to-air CO_2 and CH_4 emissions, owing to their high productivities and shallow water depths (MacLeod et al., 2020; Yuan et al., 2019). Although there have been some efforts to characterize CO_2 and CH_4 fluxes across the water-air interface and their driving variables in aquaculture ponds (e.g., Bhattacharyya et al., 2013; Chanda et al., 2019; Soares and Henry-Silva, 2019), relevant data are still scarce for China, where small-hold aquaculture ponds are widespread but poorly researched (Hu et al., 2020, 2016; Ma et al., 2018; Yuan et al., 2019, 2021; Zhang et al., 2020a). Pond drainage, a common practice done in many small-hold aquaculture ponds, may divert the carbon downstream. On the other hand, carbon sequestration in the sediment may offset the 'climate footprint' of aquaculture ponds (Boyd et al., 2010). Proper assessment of the carbon greenhouse gas emissions and global warming potential of aquaculture ponds therefore requires accounting for both carbon inputs and outputs. Yet, such a mass balance approach is rarely used in aquaculture pond studies (Zhang et al., 2020b).

In the current study, we determined the different carbon input and output components of three earthen aquaculture ponds with *Litopenaeus vannamei* within a subtropical estuary in southeastern China. The research main objectives to: (1) assess the carbon budgets of the earthen shrimp ponds, (2) quantify the contribution of CO_2 and CH_4 emissions to the total carbon output, and (3) evaluate the role of aquaculture ponds in driving global warming. We hypothesized that CO_2 and CH_4 emissions represent a major carbon loss, and the global warming effect of the shrimp ponds is on par with other food production systems. Based on the findings, we made recommendations to improve the production efficiency and minimize the climate footprint of shrimp aquaculture.

2. Materials and methods

2.1. Study area

The research was conducted in the Shanyutan Wetland (26°00′36″–26°03′42″ N, 119°34′12″–119°40′40″ E) of the Min River Estuary (MRE), southeastern China (Figure 1). It is the largest tidal wetland in the MRE, covering an area of approximately 3,120 ha. The MRE is influenced by the East Asian monsoon, with an annual average precipitation of 1,350 mm and air temperature of 19.6 °C (Tong et al., 2010). The semidiurnal tidal range is 2.5–6.0 m and the average water salinity is 4.2 ± 2.5 ‰. Aquaculture shrimp ponds, common within the Shanyutan Wetland and covering an area of ca. 234 ha (Yang et al., 2017a), were constructed by clearing away the marsh vegetation and re-profiling the bunds into slopes.

2.2. Aquaculture system and management practices

Field measurements were conducted in three coastal earthen aquaculture ponds that culture the whiteleg shrimps (*Litopenaeus vannamei*) (Figure 1). The selected ponds represent the typical management practices and physical setting of aquaculture in the MRE. They range in size of 1.25–1.40 ha and water depth of 1.3–1.6 m during the farming period (Yang et al., 2021a). The farming period is usually between 5th May and 8th November, producing a single crop. The ponds are drained and dried for the remainder of the year.

Prior to farming, the earthen ponds were filled with seawater drawn from the MRE. The seawater was first passed through a 2 mm mesh bag to exclude predators and competitors. After seven days, trichloroisocyanuric acid (~25 kg pond^{-1}) was added to disinfect the pond water, followed by the addition of calcium oxide lime (0.5 t ha^{-1}) and calcium superphosphate fertilizer (1.5–2.0 kg per 1000 m^{3}). Before shrimp stocking, probiotics (200 mL ha^{-1}) were added, and water conditions (e.g., alkalinity or acidity, salinity, etc.) were checked to make sure they were in the correct range. Each earthen pond was stocked with *L. vannamei* at a density of 215 post larvae m^{-2}. Commercial feed pellets were added daily during the farming period. Aeration was provided by aerators in the ponds. After harvesting, the pond water was discharged.

2.3. Carbon budgets of the shrimp ponds

The carbon budget was constructed by accounting for the different input and output components. Input equaled the sum of carbon input from the stocked shrimps, feeds, fertilizers, primary production of phytoplankton, inflow water and rainwater. Output equaled the sum of carbon loss through plankton respiration, sediment respiration, net carbon greenhouse gas emissions (CO_2 and CH_4), harvested shrimps, outflow water and sediment accumulation. Each of the aforementioned input and output terms was measured independently in this study, as explained below.

2.3.1. Input: Stocked shrimps and feeds

The initial stocking of shrimp biomass and daily feed amounts were recorded. Samples of the stocked shrimps and feeds were collected and oven-dried for 24 h at 60 °C (Dien et al., 2018), grounded and sieved through a 0.15 mm mesh screen, and their total carbon (TC) contents were analysed using a combustion analyzer (Elementar Vario MAX CN, Germany). The detection limit and relative standard deviations were 4 μg L^{-1} and ≤1.0% for TC, respectively.

2.3.2. Input: Primary production of phytoplankton

During each sampling campaign (May-October; 2-3 times per month), phytoplankton primary production was determined by the light−dark bottle oxygen method (Diana et al., 1991; Zhang et al., 2016, 2020b). Water samples from the surface (20 cm) and bottom (ca. 5 cm above the sediment) layers was sampled at five stations in each pond to measure the initial dissolved oxygen (DO) concentration by the Winkler method (Diana et al., 1991; Chen et al., 2018). Two dark and two light bottles (200 mL) were filled with ambient waters and suspended in situ at the original depths, and the final DO concentrations in the bottles were determined after 24 h. Gross primary production (P_P) and plankton respiration (R_P; mg O_2 L^{-1}) were calculated from the changes in DO concentrations as follows (Zhang et al., 2016):

$$P_P = DO_L - DO_L \qquad \text{(Eq.1)}$$

$$R_P = DO_I - DO_D \qquad \text{(Eq.2)}$$

where DO_L (mg L^{-1}) and DO_D (mg L^{-1}) are the final DO concentrations in the light and dark bottles, respectively; DO_I (mg L^{-1}) is the initial dissolved oxygen. Measurements were converted to carbon using the conversion of 1 mg O_2 to 0.375 mg C (Guo et al., 2017; Winberg, 1980).

2.3.3. Input: Inflow water and rainwater

Samples of inflow water were collected from two inlets using an organic glass hydrophore at each pond, while rainwater was sampled by a rain gauge 5 times during the farming period. All the water samples were stored in a cold and dark container and transferred back to laboratory for further analysis within 4–6 h. Approximately 50 mL of the water sample was filtered through a pre-combusted 0.45 μm glass fibre filter to separate the particulate organic carbon (POC) and dissolved organic carbon (DOC) fractions. Both fractions were subsequently analyzed using a total organic carbon (TOC) analyzer (TOC–$V_{CPH/CPN}$, Shimadzu, Japan). In addition, rainfall data from a local weather station were used to estimate the total precipitation entering each pond during the farming period.

2.3.4. Output: Water-column and sediment respiration

Respiration in the water column by both autotrophic and heterotrophic plankton was derived from the light-dark bottle incubations described earlier (Eq. 2) (Zhang et al., 2016, 2020b). Sediment respiration was measured with a sediment incubation chamber (30 cm length, 6 cm internal diameter; Yang et al. 2017b, 2019). Surface sediment (0-15 cm) was taken from five sites in each pond using a metal corer (diameter 6 cm). The sediment samples were sealed in vacuum inside the incubation chambers. Both sediment and pond water samples were transported to the laboratory within 4 hr, and then were allowed to equilibrate to the lab condition for 2 h (Zhang et al., 2016). The incubation chamber was filled with pond water up to 15 cm above the surface of sediment, and then sealed with a Teflon stopper. The incubation was done in an incubator (QHZ-98A, Taicang, Jiangsu, China) at in-situ temperature for 4 h in darkness. Initial and final samples of the overlying water were taken from the chamber to determine DO by Winkler titration. Incubation chambers filled with pond water only (no sediment) was used as the control. Sediment oxygen demand (SOD, mg O_2 m^{-2} d^{-1}) was determined from the change in DO in the overlying water:

$$\mathrm{SOD} = \frac{(\mathrm{DO_I} - \mathrm{DO_F}) \times V_{\mathrm{OW}}}{A_{\mathrm{SC}} \times T_{\mathrm{IE}}} \quad \text{(Eq.3)}$$

where DO_I and DO_F (mg O_2 L^{-1}) are the initial and final DO concentrations, respectively; V_{OW} (L) is the volume of overlying water in the incubation chambers, A_{SC} (m^2) is the cross-sectional area of the sediment core, T_{IE} (h) is the duration of the incubation experiment. SOD (mg O_2 m^{-2} h^{-1}) was converted to carbon demand (mg C m^{-2} d^{-1}) (1 mg O_2 = 0.375 mg C) according to Winberg (1980).

2.3.5. Output: Harvested biomass, outflow water and sediment accumulation

At the end of the farming period, the ponds were drained and the shrimps were harvested, weighed, and analyzed for TC as described above. Outflow water was collected from two outlets at each pond using an organic glass hydrophore. The water samples were analysed for POC and DOC using the same methods as described before (section 2.3.3).

Similar to previous studies (Pouil et al., 2019; Zhang et al., 2016, 2020c), carbon sedimentation was derived from sediment height accumulation over time and sediment carbon content. Briefly, five 0.5 m^2 ceramic tiles were placed inside each of the ponds at the start of the farming period, and the height of the accumulated sediment (cm) on the tiles at the end of the farming period was measured by vernier caliper. Additionally, sediment samples (0–20 cm depth) were collected on a monthly basis from five sites in each pond using a metal corer (diameter 6 cm). In the laboratory, the sediment TC were determined using an Elementar combustion analyzer (Elementar Vario MAX CN, Germany). The accumulated sediment height and sediment TC content were then used to estimate the total amount of carbon sedimentation throughout the farming period (Flickinger et al., 2020).

2.3.6. Output: Carbon greenhouse gas emissions

The fluxes of CO_2 and CH_4 across the water-air interface (WAI) were determined using the opaque floating chamber method, the details of which can be found in Natchimuthu et al. (2016). Briefly, the floating chamber had a volume of 5.2 L covering a surface area of 0.1 m^2. During each campaign, CO_2 and CH_4 flux measurements were made at five sites in each pond. At each site, gas samples were collected from the floating chamber air headspace at 0, 15, 30, and 45 min, and were then transferred into sample bags. Sampling was done between 9:00 and 11:00 local time outside of the time when the aerators were running. CO_2 and CH_4 concentrations in the gas sampled were analysed within 24 h by a gas chromatograph equipped with a flame ionization detector (GC-2010, Shimadzu, Kyoto, Japan). CH_4 fluxes determined by the floating chamber method represented the sum of ebullitive CH_4 fluxes and diffusive CH_4 fluxes (Wu et al., 2019; Zhu et al., 2016). Gas fluxes (CO_2 or CH_4; mg C m^{-2} h^{-1}) across the WAI were estimated as the rate of change in the mass of CO_2 (or CH_4) per unit surface area per unit time (Yuan et al., 2021; Zhu et al., 2016) as follows:

$$F = \frac{\mathrm{d}c}{\mathrm{d}t} \bullet \frac{M_\mathrm{M}}{V_\mathrm{M}} \bullet \frac{P}{P_0} \bullet \frac{T}{T_0 + T} \bullet H \quad \text{(Eq. 4)}$$

where F is the fluxes of CO_2 or CH_4 (mg C m^{-2} h^{-1}); dc/dt is the slope of the CO_2 (or CH_4) concentration (c, mmol mol^{-1}) curve variation over time (t, hour); M_M is the molar mass of CO_2 or CH_4 (mg mol^{-1}); V_M is the gas molar volume (m^3 mol^{-1}); P_0 and T_0 is the atmospheric pressure (kPa) and absolute temperature (K), respectively, under the standard condition; P and T is the air pressure (kPa) of the sampling pond and the air temperature (K) during the measurement, respectively; H is the floating chamber height (m) over the water surface.

2.4. Total CO_2-equivalent (CO_2-eq) emission

Because different GHGs have different degrees of radiative forcing over different time scales, to aid comparison and policy development, their respective warming effects are often expressed as CO_2-equivalent on a chosen time horizon by applying the appropriate global warming potential values (Skytt et al., 2020). In the present study, we multiplied the mass of CH_4 by a global warming potential (GWP_{20}) value of 84 to calculate its CO_2 equivalent (CO_2-eq) on a 20-year time horizon (Fang et al., 2021; IPCC, 2014). This was then added to the mass of CO_2 emission to calculate the total CO_2-eq emission on a 20-year time horizon.

2.5. Measurements of ancillary environmental variables

Meteorological data such as wind speed (W_S), air temperature (T_A), and air pressure (A_P) were measured by an automatic weather station. During field sampling at each site, we measured the hydrographical properties at 20 cm depth, including water temperature (T_W), pH, DO, and salinity. The detection limit and relative standard deviations were ±0.2 °C and ≤1.0% for T_W, 0.01 and ≤1.0% for pH, 0.1 mg L^{-1} and ≤2.0% for DO, and 0.1 ppt and ≤1.0% for salinity, respectively. Chlorophyll *a* (Chl-*a*) was measured using a spectrophotometer (Shimadzu UV-2450, Japan) following the method of Yang et al. (2017b). The nitrite-nitrogen (NO_3^--N) and ammonium-nitrogen (NH_4^+-N) concentrations were determined using a continuous flow injection analyzer (Yang et al., 2021a). The detection limits for NO_3^--N and NH_4^+-N were 0.6 μg L^{-1} and 0.6 μg L^{-1}, respectively, and the relative standard deviations were ≤2.0% and ≤3.0%, respectively.

2.6. Calculation of the carbon budget

The carbon budgets of the coastal earthen aquaculture ponds were calculated based on the mass balance (Flickinger et al., 2020; Zhang et al., 2020b) as follows:

$$IW_{in} + RW_{in} + CA_{in} + PP_{in} + FA_{in} = RPS_{out} + HA_{out} + GCE_{out} + OW_{out} + SA_{out} + UC_{out} \quad (Eq.5)$$

Among the input terms, IW_{in} is carbon input from the inflow water, RW_{in} is carbon input through rainwater, CA_{in} is the amount of carbon in stocked shrimps, PP_{in} is carbon input through phytoplankton primary production, FA_{in} is the amount of carbon in the feed. Among the output terms, RPS_{out} is carbon loss via water column respiration and sediment respiration, HA_{out} is the amount of carbon in harvested shrimps, GCE_{out} is carbon loss through carbon greenhouse gas emissions (CO_2 and CH_4), OW_{out} is carbon output from the ponds via outflow water, SA_{out} is sediment carbon accumulation, and UC_{out} is the unaccounted portion (Flickinger et al., 2020).

Carbon input from each component (IW_{in}, RW_{in}, CA_{in}, PP_{in} and FA_{in}) was estimated as the product of the carbon concentrations and the total amount of each component. Carbon output through plankton respiration in the water column were estimated as the product of the mean water depth, the R_P (Eq. 2), and the farming period (188 days). Carbon output via sediment respiration was determined as the product of the SOD (Eq. 3) and the farming period (188 days). Carbon output via HA_{out} were estimated as the product of the total harvested shrimp biomass and the carbon content of the shrimp. Carbon output via GCE_{out} across the WAI was estimated as the product of the mean carbon greenhouse gas (CO_2 and CH_4) fluxes, the pond surface area (ha), and the aquaculture period (188 days). Carbon output via OW_{out} were estimated as the product of the total amount of water discharged and the carbon concentration in the discharged water. Carbon output via SA_{out} was determined as the product of the total amount of sediment and the change in sediment carbon contents.

The environmental loading of carbon (C_{EL}, kg C t^{-1}) of the cultured shrimp was estimated as follows:

$$C_{EL} = \frac{C_E - C_I}{W_{HA}} \quad \text{(Eq.6)}$$

Where C_E is the total amount of carbon in the end of farming (kg), C_I is the total amount of carbon at the initial stage of farming (kg), and W_{HA} is the total weight of harvested shrimps (t).

2.7. Statistical analysis

Two–way analysis of variance (ANOVA) was performed to analyse the impacts of sampling ponds (Ponds I, II, and III), and time on carbon gas fluxes and total CO_2-eq emissions, with sampling sites within ponds specified as a random variable. ANOVA was also used to test for the significant differences in hydrographical properties between ponds. Pearson correlation analysis (PCA) was performed to analyse the correlations between carbon greenhouse gas emissions (CO_2 and CH_4) and environmental parameters. Redundancy analysis (RDA) was performed to evaluate which environmental parameters would best explain the variability in carbon greenhouse gas fluxes, with T_A, W_S, A_P, T_W, DO, pH, salinity, TOC, NH_4^+–N, NO_3^-–N, and Chl-*a* being included in the analysis. ANOVA and RDA were performed using SPSS 17.0 (SPSS Inc., USA) and the CANOCO 5.0 (Microcomputer Power, Ithaca, USA), respectively. Results were summarized as "mean ± 1 standard error (SE)" and the significant level was set at p = 0.05. Sampling site map, conceptual diagrams and statistical plots were created using ArcGIS 10.2 (ESRI Inc., Redlands, CA, USA), EDraw Max 7.3 (EdrawSoft, Hong Kong, China), and OriginPro 9.0 (OriginLab Corp.

USA), respectively.

3. Results

3.1. Water and sediment properties

Hydrographical properties of the three ponds during the farming period are shown in Figure 2. There were no significant differences in average T_w, DO, pH, salinity and sediment TC content were observed among the shrimp ponds (ANOVA, p>0.05; Figure 2a-d). However, significant differences were found in average total dissolved organic carbon (TOC; Figure 2e) and chlorophyll *a* (Chl-*a*; Figure 2f) among the ponds. TOC concentration in Pond II (30.9 ± 3.1 mg L^{-1}) was significantly higher than that in Pond I (20.9 ± 1.4 mg L^{-1}) and Pond III (24.3 ± 2.3 mg L^{-1}) (p>0.05; Figure 2e). The mean Chl-*a* concentration was also significantly higher in Pond II (146.9 ± 15.1 μg L^{-1}), followed by Pond I (125.4 ± 12.8 μg L^{-1}) and Pond III (116.1 ± 10.2 μg L^{-1}) ($p < 0.05$) (Figure 2f). The sediment accumulation rate across three ponds over the farming period ranged from 0.83 to 0.84 cm $month^{-1}$ (average 0.83 ± 0.01 cm $month^{-1}$). The sediment TC content across three ponds increased from an average of 16.2 ± 0.2 g kg^{-1} at the beginning of the farming period to 18.6 ± 0.1 g kg^{-1} at the end of the farming period.

3.2. Carbon greenhouse gas fluxes across the WAI

Across all sampling dates and sites, net CO_2 flux ranged from -6.8–5.3 mg C m^{-2} h^{-1} in Pond I, -8.0–5.3 mg C m^{-2} h^{-1} in Pond II and -5.8–5.8 mg C m^{-2} h^{-1} in Pond III (Figure 3a), with negative values indicating CO_2 uptake. On average, the net CO_2 flux was highest in Pond III (1.7 ± 0.9 mg C m^{-2} h^{-1}), followed by Ponds I (1.5 ± 1.0 mg C m^{-2} h^{-1}) and II (0.9 ± 1.1 mg C m^{-2} h^{-1}) (Figure 4a). Net CH_4 flux ranged 0.02–6.8, 0.2–28.1 and 0.2–39.8 mg C m^{-2} h^{-1} in Ponds I, II and III (Figure 3b), respectively. CH_4 fluxes decreased significantly in the order of Pond II (7.9 ± 1.9 mg C m^{-2} h^{-1}) > Pond III (4.2 ± 2.7 mg C m^{-2} h^{-1}) > Pond I (1.9 ± 0.5 mg C m^{-2} h^{-1}) ($p<0.01$; Figure 4b). Carbon greenhouse gas emissions varied significantly with time ($p<0.01$; Figure 3), with lower CO_2 in May-June and lower CH_4 emissions in May and October, where higher emissions of both gases were observed in August and September.

3.3. Carbon budget of the shrimp ponds

Table 1 shows the carbon inputs into the ponds. Primary production by phytoplankton (269.1–327.6 g C m^{-2}) was the largest component, accounting for 58.5–61.8% of the total input (Figure 5). Feed was the second largest component (144.9–187.3 g C m^{-2}) that accounted for 31.9–35.3% of the total input (Figure 5). Stocked shrimps, rainwater and inflow water were only minor components of the carbon budget, representing on average 0.004%, 0.4–0.5%, and 4.9–5.8% of the total input, respectively (Figure 5).

The carbon outputs of the shrimp ponds are listed in Table 2, with their relative percentages of the total output shown in Figure 5. During the farming period, the main output component was plankton respiration (231.7–243.4 g C m^{-2}), which accounted for 44.0–53.6 % of the total output. Sediment accumulation (82.0–117.6 g C m^{-2}) as the second largest component represented 18.0–21.7 % of the total output. Outflow water and biomass harvesting accounted for respectively 9.2–11.7 % and 9.0–11.4 %

of the total output. Net carbon greenhouse gas emissions across the water-air interface and sediment respiration were only minor components, equivalent to 0.8–1.6 % and 0.01–0.03 % of the total output, respectively.

3.4. Total CO_2-equivalent emission from the shrimp ponds

The combined carbon emission (CO_2 + CH_4), expressed in mg CO_2-eq m^{-2} h^{-1} based on GWP_{20}, was 221.6±61.3 in Pond I, 885.7±221.4 in Pond II, and 478.9±229.7 in Pond III (Figure 4c). Combining data from the three ponds, the mean total CO_2-equivalent emission was 528.4±193.3 mg CO_2-eq m^{-2} h^{-1}. Water-to-air CH_4 emission was the principal contributor of the total CO_2-equivalent emission, with the largest emissions observed in August–September (Figures 3c).

3.5. Effects of environmental variables on carbon greenhouse gas fluxes

Based on Pearson correlation analysis, the CO_2 fluxes were positively correlated with T_W, pH, TOC and NH_4^+-N, and negatively correlated with DO and Chl-*a* (p<0.01 or <0.05; Table 3). CH_4 fluxes were positively correlated with T_W and TOC, but negatively correlated with DO (p<0.01 or <0.05; Table 3).

According to the RDA results (Figure 6), Chl-*a*, TOC, and pH were the significant factors driving the variations in CO_2 and CH_4 fluxes (p<0.05). Among them, Chl-*a* had the highest explanatory power (51.4%), followed by TOC (30.4%) and pH (6.2%).

4. Discussion

4.1. Carbon budget of the aquaculture ponds

Primary production by phytoplankton was a main pathway for CO_2 uptake and comprised 60% of the total carbon input, which was comparable to that observed in fish aquaculture ponds (46–78 %; Zhang et al., 2016, 2020c). The estimated mean gross primary production (293 g C m^{-2}) was higher than water-column respiration (238 g C m^{-2}), causing a net autotrophic carbon fixation of ca. 55 g C m^{-2} via photosynthesis. The other main carbon input came in the form of feeds (34%; 165 g C m^{-2}). In contrast to other studies (Flickinger et al., 2020; Guo et al., 2017; Zhang et al., 2020b), inflow water accounted for only a small percentage of the carbon input in the present study (5%; 26 g C m^{-2}), largely because of the low carbon concentration in the source water. Carbon input from rainwater was negligible.

Of the total excess carbon (i.e., net autotrophic carbon fixation + feed + inflow/rain water; ca. 248 g C m^{-2}), only ca. 21% was converted to shrimp biomass (51 g C m^{-2}), showing the low efficiency of *L. vannamei* in assimilating the feeds and utilizing the carbon input for growth (cf. Flickinger et al., 2020; Zhang et al., 2016, 2020b). Sedimentation and outflow together (151 g C m^{-2}) accounted for another 61% of the total carbon output, in line with the range reported previously (Alongi et al., 2000, 2009; Sahu et al., 2013a, 2013b). Yet, net CO_2 and CH_4 emissions (13 g C m^{-2}) removed only 5% of the excess carbon, similar to that observed in other semi-intensive and intensive aquaculture systems (Flickinger et al., 2020). The higher CO_2 and CH_4 emissions observed in August-September were likely due to the higher water temperature that not only increased respiration and methanogenesis but also decreased gas solubility in the water. On average, 8.0% (range 4.2–12.6%) of the excess carbon was unaccounted for. In addition to uncertainty associated with each of the measured input and output terms, some of the missing carbon was likely associated with respiratory activities by other heterotrophs and the loss of volatile organic carbon that was not measured in this study. Furthermore, carbon loss via denitrification (Hargreaves 1998), especially in nitrate-rich system, would not be captured by our O_2-based respiration measurements.

4.2. Spatio-temporal variations in carbon greenhouse gas emissions

Large temporal variations in CO_2 and CH_4 fluxes have been found in various aquatic ecosystems, such as reservoirs (Gerardo-Nieto et al., 2017; Musenze et al., 2014), lakes (Natchimuthu et al., 2016; Xiao et al., 2021) and rivers (Luo et al., 2019; Zhao et al., 2013). However, comparable information is rare for aquaculture systems, particularly coastal earthen ponds (Chen et al., 2016; Zhang et al., 2022). Our results showed considerable temporal variations in the carbon greenhouse gas emissions from three coastal earthen shrimp ponds (Figure 3a and 3b). CO_2 and CH_4 emissions were higher in middle of the farming period (July–September) when water temperature tended to be higher than in the initial period (May–June) (Yang et al., 2021). Temperature can affect many abiotic and biotic parameters (e.g., plankton primary production, respiration, microbial activity, and nutrient availability, etc.) (Xiao et al., 2021) that in turn govern greenhouse gas production and consumption (Davidson et al., 2018; Kosten et al. 2012; Marotta et al., 2014; Rosentreter et al., 2017). Strong correlations between CO_2 (or CH_4) emissions and water temperature were observed in this study and other studies (Shaher et al., 2020; Wu et al., 2018; Zhang et al., 2022), indicating that temperature plays an important role in driving the temporal change in carbon greenhouse gas emissions from the coastal earthen aquaculture ponds.

Our results also showed substantial between-pond differences in CO_2 and CH_4 emissions (Figure 3a and 3b), with the lowest CO_2 and highest CH_4 emissions from Pond II. These variations are likely related to the differences in the physico-chemical properties of the sediment and overlying water in the ponds that influence greenhouse gas production and consumption. Among the hydrographical properties examined, only water TOC (Figure 2e), Chl-*a* (Figure 2f) and DIN (Yang et al., 2021a) differed significantly among the ponds (p<0.05 or <0.01), with the highest values observed in Pond II. An earlier study at the same site reported significantly lower shrimp survival rate (55%) and higher feed conversion rate (2.6) in Pond II than in Ponds I (65% and 1.4) and III (67% and 1.6) (Yang et al., 2021b), which might have led to the accumulation of organic matter and phytoplankton in Pond II. The high abundance of phytoplankton in Pond II, as indicated by its higher Chl-*a*, would have allowed a stronger CO_2 drawdown via photosynthesis (Davies et al., 2003; Xiao et al., 2021), and subsequently a lower net CO_2 emission from this pond. Meanwhile, the higher organic matter accumulation at Pond II could have contributed to a higher CH_4 production and emission (Davidson et al., 2018; Yang et al., 2020; Zhu et al., 2016). Despite the lack of data on the rates of microbial greenhouse gas production and consumption, the significant correlation between CO_2 emission and Chl-*a*, and between CH_4 emission and TOC (p<0.01; Table 3), implied that between-pond changes of CO_2 and CH_4 emissions were primarily driven by the availability of phytoplankton and carbon substrate (Figure 6).

4.3. Carbon greenhouse gas emission from aquaculture ponds

The average water-to-air emissions of CO_2 and CH_4 during the farming period from our ponds were within the ranges observed elsewhere (Table 4; Zhu et al., 2016; Soares and Henry-Silva, 2019; Yang et al., 2018). Although CO_2 and CH_4 emissions comprised only a small proportion of the carbon budget, the strong global warming potential of these two gases especially that of CH_4 implied that shrimp ponds could still exert a considerable impact on the climate. The estimated total CO_2-equivalent emission from the shrimp ponds averaged 528.4 ± 193.3 mg CO_2-eq m^{-2} h^{-1}, which was much higher than that reported for lakes and reservoirs in China (104.0 and 61.1 mg CO_2-eq m^{-2} h^{-1}, respectively; Li et al., 2018) and around the world (Bastviken et al., 2011; Deemer et al., 2016), but comparable to some eutrophic lakes (Sun et al., 2021; Xing et al., 2005). Assuming that our data together with the literature data (Table 4) were representative of global aquaculture ponds (110,832 km^2; Verdegem and Bosma, 2009), we estimated that aquaculture ponds would emit approximately 3.4×10^5 Gg CO_2 y^{-1} and 4.0×10^4 Gg CH_4 y^{-1} into the atmosphere. The corresponding total CO_2-equivalent emission would be 3.7×10^6 Gg CO_2-eq y^{-1}, with CH_4 as the main contributor (91%).

The growing demand for animal proteins has prompted the intensification of livestock production and aquaculture, which has raised huge concerns over their environmental impacts including greenhouse gas emissions (Godfray and Garnett, 2014). Based on our estimation, aquaculture ponds contributed only ca. 1% of the global anthropogenic CH_4 emission (Yuan et al., 2019). This was consistent with the findings of a recent meta-analysis that aquaculture has a lower greenhouse gas emission than livestock production because of the absence of enteric fermentation (a major CH_4 source in livestock) and a lower feed conversion ratio in the former (MacLeod et al., 2020).

Agriculture and livestock production are well-known sources of CH_4, contributing to about 40% of the anthropogenic CH_4 emission (Smith et al., 2008). Nevertheless, the nature and magnitude of CH_4 emission from food production systems may change as the aquaculture sector continues to expand. Based on our data, we found that the magnitude of CH_4 emission per unit area was substantially higher in aquaculture ponds (Yang et al., 2018; Yuan et al., 2021; Zhao et al., 2021) than in some agro-ecosystems such as paddy fields (e.g., Hao et al., 2016; Hou et al., 2010; Wu et al., 2018) and rice–wheat cropping systems (Guo et al., 2021; Wu et al., 2019; Yao et al., 2013), but comparable to rice-fish farming systems (e.g, Frei and Becker, 2005, Wang et al., 2019) except in India (e.g., Bhattacharyya et al., 2013; Datta et al., 2009) (Table 4). Compared to other agro-ecosystems, the large CH_4 flux observed in aquaculture ponds may be the result of high sediments organic matter and the continuously flooded environment that would favor CH_4 production and ebullition (Davidson et al., 2018; Yang et al., 2020).

Based on the results of the carbon budget, we could identify possible ways to reduce the climate footprint of aquaculture. Given that only 21% of the excess carbon was converted to shrimp biomass, the majority of the excess carbon would end up in various parts of the ponds (e.g. surface water) and adjacent ecosystems. By improving feed formulation and feed management, shrimp farmers could decrease the feed conversion ratio, increase the production efficiency and minimize waste generation (White, 2013). We also found that a large proportion (20%) of the excess carbon eventually accumulated in the sediment, which could promote anoxia and methanogenesis if left untreated. Sediment removal between farming seasons by dredging is not a common practice among the local shrimp farmers, but it could be a simple and effective strategy to mitigate greenhouse gas emissions, with the added benefits of utilizing the organic-rich sediment as fertilizers (Pouil et al., 2019).

4.4. Limitation and future outlook

There were some limitations in our study. Firstly, we examined the carbon budget of shrimp ponds located in one estuary only during the farming period. Scaling up our data from the local to the regional scale may increase the uncertainty of budget calculation. To further improve the carbon budget accuracy at the regional and global scales, more studies on other variables such as aquaculture operation types, farmed species and management practice, are required. Secondly, this study only considered the major gains and losses of carbon. However, ~4.2–12.6% of the carbon output was missing from the budget (Figure 5), which can be attributed to a combination of uncertainty associated with the measurements and carbon loss processes that were not captured by our methods. Some studies have shown that farmed animals' respiration could account for approximately 1.3–3.6% of the carbon loss (Xia et al., 2013; Zhang 2019); periphyton respiration is another potential contributor of carbon output (Zhang et al., 2016). However, these processes can be patchy and may not be properly captured by floating chamber measurements. Future studies should consider quantifying the respiration by the farmed animals and periphyton. Anaerobic respiration, which can be important in nitrate-rich aquaculture ponds (Hargreaves 1998), can be better quantified by direct CO_2 measurements. Lastly, we measured carbon greenhouse gas emissions only during the daytime, whereas the diel variations of gaseous carbon fluxes might introduce some uncertainties to our carbon budget. Meanwhile, some pond management practices such as aeration and drainage activities could affect carbon emissions from aquaculture ponds (Datta et al., 2009; Kosten et al., 2020). Our present study was limited to the farming period when aeration was routinely applied to the ponds; therefore, the carbon emission measurements may not be representative of the situation where aeration is not used. To obtain accurate estimates of annual emissions, more detailed investigation of carbon emission during the dry-period (or non-farming period) and in non-aerated system/ period is needed (Kosten et al., 2020).

5. Conclusion

The present study adopted a carbon budget approach to investigate the major inputs and outputs of carbon in three coastal aquaculture ponds with *L. vannamei* in the MRE in southeastern China. In situ plankton production and respiration were the main components of the carbon flows. Overall, water-to-air CO_2 and CH_4 emissions were relatively small contributions to the carbon budget, but the CH_4 emission was still higher than that in other agro-ecosystems. We showed that the use of a mass balance approach can provide useful insights into the carbon budget and dynamics within the aquaculture ponds and help identify ways to improve production efficiency and reduce the climate footprint of aquaculture production.

Acknowledgments

This work was funded by the National Natural Science Foundation of China (NSFC) (grant numbers 41801070 and 41671088), and the Natural Science Foundation of Fujian Province of China (grant numbers 2020J01136 and 2018J01737). We are grateful to members from Research Centre of Wetlands in Subtropical Region led by Dr. Chuan Tong at Fujian Normal University and staff at Minjiang Estuary Wetland National Nature Reserve for their help in the fieldwork. We thank the Editor and two anonymous Reviewers for the very helpful comments.

References

Alongi, D.M., Johnston, D.J., Xuan, T.T., 2000. Carbon and nitrogen budgets in shrimp ponds of extensive mixed shrimp–mangrove forestry farms in the Mekong Delta, Vietnam. Aquac. Res. 31, 387–399.

Alongi, D.M., McKinnon, A.D., Brinkman, R., Trott, L.A., Undu, M.C., Rachmansyah, M., 2009. The fate of organic matter derived from small-scale fish cage aquaculture in coastal waters of Sulawesi and Sumatra, Indonesia. Aquaculture 295, 60–75.

Bastviken, D., Tranvik, L.J., Downing, J.A., Crill, P.M., Enrich-Prast, A., 2011. Freshwater methane emissions offset the continental carbon sink. Science 331, 50. https://doi.org/10.1126/science.1196808

Bhattacharyya, P., Sinhababu, D.P., Roy, K.S., Dash, P.K., Sahu, P.K., Dandapat, R., Neogi, S., Mohanty, S., 21013. Effect of fish species on methane and nitrous oxide emission in relation to soil C, N pools and enzymatic activities in rainfed shallow lowland rice-fish farming system. Agr. Ecosyst. Environ. 176, 53-62. https://doi.org/10.1016/j.agee.2013.05.015

Boyd, C.E., Wesley Wood, C., Chaney, P.L., Queiroz, J.F., 2010. Role of aquaculture pond sediments in sequestration of annual global carbon emissions. Environ. Pollut. 158, 2537–2540. https://doi.org/10.1016/j.envpol.2010.04.025

Chanda, A., Das, S., Bhattacharyya, S., Das, I., Giri, S., Mukhopadhyay, A., Samanta, S., Dutta, D., Akhand, A., Choudhury, S.B., Hazra, S., 2019. CO_2 fluxes from aquaculture ponds of a tropical wetland: Potential of multiple lime treatment in reduction of CO_2 emission. Sci. Total Environ. 655, 1321–1333. https://doi.org/10.1016/j.scitotenv.2018.11.332

Chen, Y., Dong, S.L., Wang, F., Gao, Q.F., Tian, X.L., 2016. Carbon dioxide and methane fluxes from feeding and no-feeding mariculture ponds. Environ. Pollut. 212, 489–497. http://dx.doi.org/10.1016/j.envpol.2016.02.039

Chen, Y., Dong, S.L., Bai, Y.C., Xu, S.G., Yang, X.F., Pan, Z., 2018. Carbon budgets from mariculture ponds without a food supply. Aquacult. Environ. Interact. 10, 465–472. https://doi.org/10.3354/aei00279

Datta, A., Nayak, D.R., Sinhababu, D.P., Adhya, T.K., 2009. Methane and nitrous oxide emissions from an integrated rainfed rice–fish farming system of Eastern India. Agr. Ecosyst. Environ. 129(1-3), 228-237. https://doi.org/10.1016/j.agee.2008.09.003

Davidson, T.A., Audet, J., Jeppesen, E., Landkildehus, F., Lauridsen, T.L., Søndergaard, M., Syväranta, J., 2018. Synergy between nutrients and warming enhances methane ebullition from experimental lakes. Nat. Clim. Change 8 (2), 156. https://doi.org/10.1038/s41558-017-0063-z

Davies, J.M., Hesslein, R.H., Kelly, C.A., Hecky, R.E., 2003. $p\text{CO}_2$ method for measuring photosynthesis and respiration in freshwater lakes. J. Plankton Res. 25, 385–395. https://doi.org/10.1093/plankt/25.4.385

Diana, J.S., Lin, C.K., Schneeberger, P.J., 1991. Relationships among nutrient inputs, water nutrient concentrations, primary production, and yield of Oreochromis niloticus in ponds. Aquaculture 92, 323–341.

Deemer, B.R., Harrison, J.A., Li, S., Beaulieu, J.J., Delsontro, T., Barros, N., BezerraNeto, J.F., Powers, S.M., dos Santos, M.A., Vonk, J.A., 2016. Greenhouse gas emissions from reservoir water surfaces: a new global synthesis. Bioscience 66, 949–964. https://doi.org/10.1093/biosci/biw117

Dien, L.D., Hiep, L.H., Hao, N.V., Sammut, J., Burford, M.A., 2018. Comparing nutrient budgets in integrated rice-shrimp ponds and shrimp grow-out ponds. Aquaculture 484, 250–258. https://doi.org/10.1016/j.aquaculture.2017.11.037

FAO, 2018. The State of World Fisheries and Aquaculture. Food and Agricultural Organization of the United Nations, Rome, Italy.

Fang, K.K., Gao, H., Sha, Z.M., Dai, W., Yi, X.M., Chen, H.Y., Cao, L.K., 2021. Mitigating global warming potential with increase net ecosystem economic budget by integrated rice-frog farming in eastern China. Agr. Ecosyst. Environ. 308, 107235. https://doi.org/10.1016/j.agee.2020.107235

Fang, X.T., Zhao, J.T., Wu, S., Yu, K., Huang, J., Ding, Y., Hu, T., Xiao, S.Q., Liu, S.W., Zou, J.W., 2022. A two-year measurement of methane and nitrous oxide emissions from freshwater aquaculture ponds: Affected by aquaculture species, stocking and water management. Sci. Total Environ. 813, 151863. https://doi.org/10.1016/j.scitotenv.2021.151863

Flickingera, D.L., Costa, G.A., Dantas, D.P., Proença, D.C., David, F.S., Durborow, R.M., Moraes-Valentia, P., Valenti, W.C., 2020. The budget of carbon in the farming of the Amazon river prawn and tambaqui fish in earthen pond monoculture and integrated multitrophic systems. Aquacult. Rep. 17, 100340. https://doi.org/10.1016/j.aqrep.2020.100340

Frei, M., Becker, K., 2005. Integrated rice-fish production and methane emission under greenhouse conditions. Agr. Ecosyst. Environ. 107, 51–56. https://doi.org/10.1016/j.agee.2004.10.026

Frei, M., Razzak, M.A., Hossain, M.M., Oehme, M., Dewan, S., Becker, K., 2007. Methane emissions and related physicochemical soil and water parameters in rice–fish systems in Bangladesh. Agr. Ecosyst. Environ. 120(2–4), 391–398. https://doi.org/10.1016/j.agee.2006.10.013

Gerardo-Nieto, O., Astorga-Espana, M.S., Mansilla, A., Thalasso, F., 2017. Initial report on methane and carbon dioxide emission dynamics from sub-Antarctic freshwater ecosystems: a seasonal study of a lake and a reservoir. Sci. Total Environ. 593, 144–154. https://doi.org/10.1016/j.scitotenv.2017.02.144

Godfray, H.C.J., Garnett, T., 2014. Food security and sustainable intensification. Philos. T. R. Soc. B. 369(1639), 20120273. https://doi.org/10.1098/rstb.2012.0273

Guo, L.J., Zhang, L., Liu, L., Sheng, F., Cao, C.G., Li, C.F., 2021. Effects of long-term no tillage and straw return on greenhouse gas emissions and crop yields from a rice-wheat system in central China. Agr. Ecosyst. Environ. 322, 107650. https://doi.org/10.1016/j.agee.2021.107650

Guo, K., Zhao, W., Jiang, Z.Q., Dong, S.L., 2017. A study of organic carbon, nitrogen and phosphorus budget in jellyfish-shellfish-fish-prawn polyculture ponds. Aquac. Res. 48, 68–76. https://doi.org/10.1111/are.12861

Hao, Q.J., Jiang, C.S., Chai, X.S., Huang, Z., Fan, Z.W., Xie, D.T., He, X.H., 2016. Drainage, no-tillage and crop rotation decreases annual cumulative emissions of methane and nitrous oxide from a rice field in Southwest China. Agr. Ecosyst. Environ. 233, 270–281. https://doi.org/10.1016/j.agee.2016.09.026

Hargreaves, J.A., 1998. Nitrogen biogeochemistry of aquaculture ponds. Aquaculture 166(3-4), 181-212. https://doi.org/10.1016/S0044-8486(98)00298-1

Hou, H.J., Peng, S.Z., Xu, J.Z., Yang, S.H., Mao, Z., 2010. Seasonal variations of CH_4 and N_2O emissions in response to water management of paddy fields located in Southeast China. Chemosphere 89, 884–892. http://dx.doi.org/10.1016/j.chemosphere.2012.04.066

Hu, B.B., Xu, X.F., Zhang, J.F., Wang, T.L., Meng, W.Q., Wang, D.Q., 2020. Diurnal variations of greenhouse gases emissions from reclamation mariculture ponds. Estuar. Coastal Shelf S. 237, 106677. https://doi.org/10.1016/j.ecss.2020.106677

Hu, Z.Q., Wu, S., Ji, C., Zou, J.W., Zhou, Q.S., Liu, S.W., 2016. A comparison of methane emissions following rice paddies conversion to crab-fish farming wetlands in southeast China. Environ. Sci. Pollut. R. 23(2), 1505-1515.

IPCC, 2014. Climate change 2014: mitigation of climate change. Contribution of Working Group III to the Fifth Assessment Report of the Intergovernmental Panel on Climate Change. Cambridge University Press, Cambridge.

IPCC, 2019. In: Calvo Buendia, E., Tanabe, K., Kranjc, A., Baasansuren, J., Fukuda, M., Ngarize, S. (Eds.), 2019 Refinement to the 2006 IPCC Guidelines for National Greenhouse Gas Inventories, Volum 4. IPCC, Switzerland. Kanagawa, Japan Chapter 07.

Kim, D.G., Kirschbaum, M.U.F., 2015. The effect of land-use change on the net exchange rates of greenhouse gases: A compilation of estimates. Agr. Ecosyst. Environ. 208, 114–126. https://doi.org/10.1016/j.agee.2015.04.026

Kosten, S., Huszar, V.L.M., Bécares, E., Costa, L.S., van Donk, E., Hansson, L.-A., Jeppesen, E., Kruk, C., Lacerot, G., Mazzeo, N., De Meester, L., Moss, B., Lürling, M., Nõges, T., Romo, S., Scheffer, M., 2012. Warmer climates boost cyanobacterial dominance in shallow lakes. Glob. Chang. Biol. 18, 118–126. https://doi.org/10.1111/j.1365-2486.2011.02488.x

Kosten, S., Almeida, R.M., Barbosa, I., Mendonça, R., Muzitano, I.S., Oliveira-Junior, E.S., Vroom, R.J.E., Wang, H.J., Barros, N., 2020. Better assessments of greenhouse gas emissions from global fish ponds needed to adequately evaluate aquaculture footprint. Sci. Total Environ. 748, 141247. https://doi.org/10.1016/j.scitotenv.2020.141247

Li, S.Y., Bush, R.T., Santos, I.R., Zhang, Q., Song, K.S., Mao, R., Wen, Z.D., Lu, X.X. 2018. Large greenhouse gases emissions from China's lakes and reservoirs. Water Res. 147, 13–24. https://doi.org/10.1016/j.watres.2018.09.053

Luo, J.C., Li, S.Y., Ni, M.F., Zhang, J., 2019. Large spatiotemporal shifts of CO_2 partial pressure and CO_2 degassing in a monsoonal headwater stream. J. Hydrol. 579, 124135. https://doi.org/10.1016/j.jhydrol.2019.124135

Ma, Y.C., Sun, L.Y., Liu, C.Y., Yang, X.Y., Zhou, W., Yang, B., Schwenke, G., Liu, D.L., 2018. A comparison of methane and nitrous oxide emissions from inland mixed-fish and crab aquaculture ponds. Sci. Total Environ. 637–638, 517–523. https://doi.org/10.1016/j.scitotenv.2018.05.040

MacLeod, M.J., Hasan, M.R., Robb, D.H.F., Mamun-Ur-Rashid, M., 2020. Quantifying greenhouse gas emissions from global aquaculture. Sci. Rep. 10, 11679. https://doi.org/10.1038/s41598-020-68231-8

Marotta, H., Pinho, L., Gudasz, C., Bastviken, D., Tranvik, L.J., Enrich-Prast, A., 2014. Greenhouse gas production in low-latitude lake sediments responds strongly to warming. Nat. Clim. Change 4, 467–470. https://doi.org/10.1038/nclimate2222

Musenze, R.S., Grinham, A., Werner, U., Gale, D., Sturm, K., Udy, J., Yuan, Z.G., 2014. Assessing the spatial and temporal variability of diffusive methane and nitrous oxide emissions from subtropical freshwater reservoirs. Environ. Sci. Technol. 48, 14499–14507. https://doi.org/10.1021/es505324h

Natchimuthu, S., Sundgren, I., Gålfalk, M., Klemedtsson, L., Crill, P., Danielsson, Å., Bastviken, D., 2016. Spatio-temporal variability of lake CH_4 fluxes and its influence on annual whole lake emission estimates. Limnol. Oceanogr. 61(S1), S13-S26. https://doi.org/10.1002/lno.10222

NOAA (National Oceanic and Atmospheric Administration), 2022. Carbon cycle greenhouse gases: Trends in CH_4. Available in: https://www.esrl.noaa.gov/gmd/ccgg/trends_ch4/

Pouil, S., Samsudin, R., Slembrouck, J., Sihabuddin, A., Sundari, G., Khazaidan, K., Kristanto, A. H., Pantjara, B., Caruso, D., 2019. Nutrient budgets in a small-scale freshwater fish pond system in Indonesia. Aquaculture 504, 267-274. https://doi.org/10.1016/j.aquaculture.2019.01.067

Ren, C.Y., Wang, Z.M., Zhang, Y.Z., Zhang, B., Chen, L., Xia, Y.B., Xiao, X.M., Doughty, R.B., Liu, M.Y., Jia, M., Mao, D.H., Song, K.S., 2019. Rapid expansion of coastal aquaculture ponds in China from Landsat observations during 1984–2016. Int. J. Appl. Earth Obs. 82, 101902. https://doi.org/10.1016/j.jag.2019.101902

Rosentreter, J.A., Maher, D.T., Ho, D.T., Call, M., Barr, J.G., Eyre, B.D., 2017. Spatial and temporal variability of CO_2 and CH_4 gas transfer velocities and quantification of the CH_4 microbubble flux in mangrove dominated estuaries. Limnol. Oceanogr. 62(2), 561–578. https://doi.org/10.1002/lno.10444

Shaher, S., Chanda, A., Das, S., Das, I., Giri, S., Samanta, S., Hazra, S., Mukherjee, A.D., 2020. Summer methane emissions from sewage waterfed tropical shallow aquaculture ponds characterized by different water depths. Environ. Sci. Pollut. Res. 27(15), 18182–18195. https://doi.org/10.1007/s11356-020-08296-0

Sahu, B.C., Adhikari, S., Dey, L., 2013a. Carbon, nitrogen and phosphorus budget in shrimp (*Penaeus monodon*) culture ponds in eastern India. Aquac. Int. 21, 453–466. https://doi.org/10.1080/10454438.2015.1115320

Sahu, B.C., Adhikari, S., Mahapatra, A.S., Dey, L., 2013b. Carbon, nitrogen, and phosphorus budget in scampi (*Macrobrachium rosenbergii*) culture ponds. Environ. Monit. Assess. 185, 10157-10166. https://doi.org/10.1007/s10661-013-3320-2

Shen, J.L., Tang, H., Liu, J.Y., Wang, C., Li,Y., Ge, T.D., Jones, D.L., Wu, J.S., 2014. Contrasting effects of straw and straw-derived biochar amendments on greenhouse gas emissions within double rice cropping systems. Agr. Ecosyst. Environ. 188, 264–274. http://dx.doi.org/10.1016/j.agee.2014.03.002

Smith, P., Martino, D., Cai, Z., Gwary, D., Janzen, H., Kumar, P., McCarl, B., Ogle, S., O'Mara, F., Rice, C., Scholes, B., Sirotenko, O., Howden, M., McAllister, T., Pan, G.X., Romanenkov, V., Schneider, U., Towprayoon, S., Wattenbach, M., Smith, J., 2008. Greenhouse gas mitigation in agriculture. Philos. T. R. Soc. B 363 (1492), 789–813.

https://doi.org/10.1098/rstb.2007.2184

Soares, D.C.E., Henry-Silva, G.G., 2019. Emission and absorption of greenhouse gases generated from marine shrimp production (*Litopeneaus vannamei*) in high salinity. J. Clean. Prod. 218, 367–376. https://doi.org/10.1016/j.jclepro.2019.02.002

Skytt, T., Nielsen, S.N., Jonsson, B.G., 2020. Global warming potential and absolute global temperature change potential from carbon dioxide and methane fluxes as indicators of regional sustainability–A case study of Jämtland, Sweden. Ecol. Indic. 110, 105831. https://doi.org/10.1016/j.ecolind.2019.105831

Sun, H.Y., Lu, X.X., Yu, R.H., Yang, J., Liu, X.Y., Cao, Z.X., Zhang, Z.Z., Li, M.X., Geng, Y., 2021. Eutrophication decreased CO_2 but increased CH_4 emissions from lake: A case study of a shallow Lake Ulansuhai. Water Res. 201, 117363. https://doi.org/10.1016/j.watres.2021.117363

Tong, C., Wang, W.Q., Zeng, C.S., Marrs, R., 2010. Methane emissions from a tidal marsh in the Min River estuary, southeast China. J. Environ. Sci. Heal. A. 45, 506–516. https://doi.org/10.1080/10934520903542261

Tranvik, L.J., Downing, J.A., Cotner, J.B., Loiselle, S.A., Striegle, R.G., Ballatore, T.J., Dillon, P., Finlay, K., Fortino, K., Knoll, L.B., Kortelainen, P.L., Kutser, T., Larsen, S., Laurion, I., Leech, D.M., McCallister, S.L., McKnight, D.M., Melack, J.M., Overholt, E., Porter, J.A., Prairie, Y., Renwick, W.H., Roland, F., Sherman, B.S., Schindler, D.W., Sobek, S., Tremblay, A., Vanni, M.J., Verschoor, A.M., von Wachenfeldt, E., Weyhenmeyera, G.A., 2009. Lakes and reservoirs as regulators of carbon cycling and climate. Limnol. Oceanogr. 54(6), 2298–2314. https://doi.org/10.4319/lo.2009.54.6_part_2.2298

Verdegem, M.C.J., Bosma, R.H., 2009. Water withdrawal for brackish and inland aquaculture, and options to produce more fish in ponds with present water use. Water Policy 11, 52–68.

Wang, A., Ma, X.Z., Xu, J., Lu, W.Q., 2019. Methane and nitrous oxide emissions in rice-crab culture systems of northeast China. Aquacult. Fish. 4(4), 134–141. https://doi.org/10.1016/j.aaf.2018.12.006

White, P., 2013. Environmental consequences of poor feed quality and feed management. FAO Fisheries and Aquaculture Technical Paper, 583, 553–564.

Winberg, G.G., 1980. General characteristics of freshwater ecosystems based on Soviet IBP studies. The Functioning of Freshwater Ecosystems. Cambridge University Press, London, pp. 481–491.

Wu, S., Li, S.Q., Zou, Z.H., Hu, T., Hu, Z.Q., Liu, S.W., Zou, J.W., 2019. High methane emissions largely attributed to ebullitive fluxes from a subtropical river draining a rice paddy watershed in China. Environ. Sci. Technol. 53, 349–3507. https://doi.org/10.1021/acs.est.8b05286

Wu, S., Hu, Z.Q., Hu, T., Chen, J., Yu, K., Zou, J.W., Liu, S.W., 2018b. Annual methane and nitrous oxide emissions from rice paddies and inland fish aquaculture wetlands in Southeast China. Atmos. Environ. 175, 135–144. https://doi.org/10.1016/j.atmosenv.2017.12.008

Wu, Z., Zhang, X., Dong, Y.B., Li, B., Xiong, Z.Q., 2019. Biochar amendment reduced greenhouse gas intensities in the rice-wheat rotation system: six-year field observation and meta-analysis. Agr. Forest Meteorol. 278, 107625. https://doi.org/10.1016/j.agrformet.2019.107625

Xia, B., Gao, Q.F., Dong, S.L., Shin, P.K.S., Wang, F., 2013. Uptake of farming wastes by silver carp *Hypophthalmichthys molitrix* in polyculture ponds of grass carp *Ctenopharyngodon idella*: evidence from C and N stable isotopic analysis. Aquaculture 404–405, 8–14.

Xiao, Q.T., Duan, H.T., Qin, B.Q., Hu, Z.H., Zhang, M., Qi, T.C., Lee, X.H., Eutrophication and temperature drive large variability in carbon dioxide from China's Lake Taihu. Limnol. Oceanogr. 9999, 1–13. https://doi.org/10.1002/lno.11998

Xing, Y.P., Xie, P., Yang, H., Ni, L.Y., Wang, Y.S., Rong, K.W., 2005. Methane and carbon dioxide fluxes from a shallow hypereutrophic subtropical Lake in China. Atmos. Environ. 39(30), 5532–5540. https://doi.org/10.1016/j.atmosenv.2005.06.010

Yang, H., Xie, P., Ni, L., Flower, R.J., 2011. Underestimation of CH_4 emission from freshwater lakes in China. Environ. Sci. Technol. 45, 4203-4204. https://doi.org/10.1021/es2010336

Yang, P., Bastviken, D., Jin, B.S., Mou, X.J., Tong, C., 2017a. Effects of coastal marsh conversion to shrimp aquaculture ponds on CH_4 and N_2O emissions. Estuar. Coast. Shelf S. 199, 125–131. https://doi.org/10.1016/j.ecss.2017.09.023

Yang, P., Lai, D.Y.F., Jin, B.S., Bastviken, D., Tan, L.S., Tong, C., 2017b. Dynamics of dissolved nutrients in the aquaculture shrimp ponds of the Min River estuary, China: Concentrations, fluxes and environmental loads. Sci. Total Environ. 603–604, 256–267. http://dx.doi.org/10.1016/j.scitotenv.2017.06.074

Yang, P., Laid, D.Y.F., Yang, H., Tong, C., 2019. Carbon dioxide dynamics from sediment, sediment-water interface and overlying water in the aquaculture shrimp ponds in subtropical estuaries, southeast China. J. Environ. Manage. 236, 224–235. https://doi.org/10.1016/j.jenvman.2019.01.088

Yang, P., Zhang, Y.F, Lai, D.Y.F., Tan, L.S., Jin, B.S., Tong, C., 2018. Fluxes of carbon dioxide and methane across the water–atmosphere interface of aquaculture shrimp ponds in two subtropical estuaries: The effect of temperature, substrate, salinity and nitrate. Sci. Total Environ. 635, 1025–1035. https://doi.org/10.1016/j.scitotenv.2018.04.102

Yang, P., Zhang, Y.F., Yang, H., Guo, Q.Q., Lai, D.Y.F., Zhao, G.H., Li, L., Tong, C., 2020. Ebullition was a major pathway of methane emissions from the aquaculture ponds in southeast China. Water Res. 184, 116176. https://doi.org/10.1016/j.watres.2020.116176

Yang, P., Zhao, G.H., Tong, C., Tang, K.W., Lai, D.Y.F., Li, L., Tang, C., 2021a. Assessing nutrient budgets and environmental impacts of coastal land-based aquaculture system in southeastern China. Agr. Ecosyst. Environ. 322, 107662. https://doi.org/10.1016/j.agee.2021.107662

Yang, P., Huang, J.F., Tan, L.S., Tong, C., Jin, B.S., Hu, B.B., Gao, C.J., Yuan, J.J., Lai, D.Y.F., Yang, H., 2021b. Large variations in indirect N_2O emission factors (EF_5) from coastal aquaculture systems in China from plot to regional scales. Water Res. 200, 117208. https://doi.org/10.1016/j.watres.2021.117208

Yang, P., Huang J.F., Yang H., Peñuelas J., Tang K.W., Lai D.Y.F., Wang D.Q., Xiao Q.T., Sardans J., Zhang Y.F., Tong C., 2021. Diffusive CH_4 fluxes from aquaculture ponds using floating chambers and thin boundary layer equations. Atmosp. Environ. 253, 118384. https://doi.org/10.1016/j.atmosenv.2021.118384

Yao, Z.S., Zheng, X.H., Dong, H.B., Wang, R., Mei, B.L., Zhu, J.G., 2012. A 3-year record of N_2O and CH_4 emissions from a sandy loam paddy during rice seasons as affected by different nitrogen application rates. Agr. Ecosyst. Environ. 152, 1–9. https://doi.org/10.1016/j.agee.2012.02.004

Yao, Z.S., Zheng, X.H., Wang, R., Xie, B.H., Butterbach-Bahl, K., Zhu, J.G., 2013. Nitrous oxide and methane fluxes from a rice–wheat crop rotation under wheat residue incorporation and no-tillage practices. Atmos. Environ. 79, 641–649. https://doi.org/10.1016/j.atmosenv.2013.07.006

Yuan, J.J., Liu, D.Y., Xiang, J., He, T.H., Kang, H., Ding, W.X., 2021. Methane and nitrous oxide have separated production zones and distinct emission pathways in freshwater aquaculture ponds. Water Res. 190, 116739. https://doi.org/10.1016/j.watres.2020.116739

Yuan, J.J., Xiang, J., Liu, D.Y., Kang, H., He, T.H., Kim, S., Lin, Y.X., Freeman, C., Ding, W.X., 2019. Rapid growth in greenhouse gas emissions from the adoption of industrial-scale aquaculture. Nat. Clim. Change 9 (4), 318–322. https://doi.org/10.1038/s41558-019-0425-9

Zhang, D.X., 2019. The carbon budgets in different aquaculture systems of *Sebastes schlegelii* and *Chlamys Farreri*. In: Study on the Impact of Chlamys farreri on the Carbon Sink/Source Function of Different *Sebastes schlegelii* and *Chlamys farreri* Aquaculture Systems 86. Ocean University of China Press.

Zhang, D.X., Tian, X.L., Dong, S,L., Chen, Y., Feng, J., He, R.P., Zhang, K., 2020a. Carbon dioxide fluxes from two typical mariculture polyculture systems in coastal China. Aquaculture 521, 735041. https://doi.org/10.1016/j.aquaculture.2020.735041

Zhang, D.X., Tian, X.L., Dong, S.L., Chen, Y., Feng, J., He, R. P., Zhang, K., 2020b. Carbon budgets of two typical polyculture pond systems in coastal China and their potential roles in the global carbon cycle. Aquacult. Environ. Interact. 12, 105–115. https://doi.org/10.3354/aei00349

Zhang, K., Yu, D.G., Li, Z.F., Xie, J., Wang, G.J., Gong, W.B., Yu, E.M., Tian, J.J., 2020c. Influence of eco-substrate addition on organic carbon, nitrogen and phosphorus budgets of intensive aquaculture ponds of the Pearl River, China. Aquaculture 520, 734868. https://doi.org/10.1016/j.aquaculture.2019.734868

Zhang, K., Tian, X.L., Dong, S.L., Feng, J., He, R.P., 2016. An experimental study on the budget of organic carbon in polyculture systems of swimming crab with white shrimp and short-necked clam. Aquaculture 451, 58–64. http://dx.doi.org/10.1016/j.aquaculture.2015.08.029

Zhao, J.Y., Zhang, M., Xiao, W., Jia, L., Zhang, X.F., Wang, J., Zhang, Z., Xie, Y.H., Pu, Y.N., Liu, S.D., Feng, Z.Z., Lee, X.H., 2021. Large methane emission from freshwater aquaculture ponds revealed by long-term eddy covariance observation. Agr. Forest Meteorol. 308–309, 108600. https://doi.org/10.1016/j.agrformet.2021.108600

Zhao, Y., Wu, B.F., Zeng, Y., 2013. Spatial and temporal patterns of greenhouse gas emissions from Three Gorges Reservoir of China. Biogeosciences, 10(2), 1219–1230. https://doi.org/10.5194/bg-10-1219-2013

Zhu, D., Wu, Y., Chen, H., He, Y. X., Wu, N., 2016. Intense methane ebullition from open water area of a shallow peatland lake on the eastern Tibetan Plateau. Sci. Total Environ. 542, 57–64. https://doi.org/10.1016/j.scitotenv.2015.10.087

Zhu, L., Che, X., Liu, H., Liu, X.G., Liu, C., Chen, X.L., Shi, X., 2016. Greenhouse gas emissions and comprehensive greenhouse effect potential of *Megalobrama amblycephala* culture pond ecosystems in a 3-month growing season. Aquac. Int. 24 (4), 893–902. https://doi.org/10.1007/s10499-015-9959-7

Zhang, Y.P., Qin, Z.C., Li, T.T., Zhu, X.D., 2022. Carbon dioxide uptake overrides methane emission at the air-water interface of algae-shellfish mariculture ponds: Evidence from eddy covariance observations. Sci. Total Environ. 815, 152867. http://dx.doi.org/10.1016/j.scitotenv.2021.152867

Zhang, L., Zheng, J.C., Chen, L.G., Shen, M.X., Zhang, X., Zhang, M.Q., Bian, X.M., Zhang, J., Zhang, W.J., 2015. Integrative effects of soil tillage and straw management on crop yields and greenhouse gas emissions in a rice–wheat cropping system. Eur. J. Agron. 63, 47–54. https://doi.org/10.1016/j.eja.2014.11.005

Table 1

Carbon inputs (g C m^{-2}) into the three aquaculture ponds with *Litopenaeus vannamei* during the farming period.

Pond	Inflow water	Rainwater	Stocked biomass	Primary production	Feed	Total
I	26.40	2.27	0.02	280.80	144.90	454.39
II	26.40	2.23	0.02	327.60	187.26	543.51
III	26.40	2.23	0.02	269.10	162.29	460.04
Mean	26.40	2.24	0.02	292.50	164.82	485.98

Table 2

Carbon outputs (g C m^{-2}) from the three aquaculture ponds with *Litopenaeus vannamei* during the farming period.

Pond	Respiration		Harvested biomass	Water-to-air emission		Outflow water	Sediment accumulation	Total	Others
	Water column	Sediment		CO_2	CH_4				
I	243.36	0.03	40.89	1.5	1.9	53.26	81.98	422.92	31.47
II	239.01	0.01	59.77	0.9	7.9	49.88	117.65	475.12	68.39
III	231.66	0.03	52.34	1.7	4.2	51.39	99.22	440.54	19.50
Mean	238.01	0.02	51.00	1.37	4.67	51.51	99.62	446.20	39.78

Table 3

Correlation coefficient matrix of carbon greenhouse gas fluxes (CO_2 and CH_4) and different environmental variables for the coastal aquaculture ponds with *Litopenaeus vannamei* during the farming period. Symbols * and ** represent the significant levels at $p < 0.05$ and $p < 0.01$.

	CO_2 flux	**CH_4 flux**	**T_A**	**A_P**	**W_S**	**T_W**	**DO**	**pH**	**Salinity**	**TOC**	**NO_3^--N**	**NH_4^+-N**	**Chl-*a***
CO_2 flux	1	0.273	0.090	0.015	-0.276	0.330*	-0.474**	0.406**	-0.061	0.440**	0.258	0.399**	-0.799**
CH_4 flux		1	0.207	-0.127	-0.160	0.353*	-0.478**	0.078	-0.133	0.757**	0.134	-0.080	-0.036
T_A			1	-0.804**	0.181	0.894**	-0.051	0.128	-0.184	0.104	-0.084	-0.532**	-0.034
A_P				1	-0.277	-0.781**	0.118	0.147	0.259	-0.094	0.257	0.619**	0.115
W_S					1	0.036	0.061	-0.109	0.018	-0.276	-0.203	-0.296*	0.056
T_W						1	-0.233	0.214	-0.308*	0.277	-0.037	-0.398**	-0.266
DO							1	-0.152	-0.032	-0.599**	-0.151	-0.069	0.457**
pH								1	0.045	0.129	0.326*	0.231	-0.129
Salinity									1	0.182	0.192	0.088	0.143
TOC										1	0.365*	0.037	-0.203
NO_3^--N											1	0.433**	-0.142
NH_4^+-N												1	-0.259
Chl-*a*													1

T_A, A_P, W_S, T_W, DO, TOC and Chl-*a* represent air temperature, atmospheric pressure, wind speed, water temperature, dissolved oxygen, total organic carbon and chlorophyll *a*, respectively.

Table 4

Comparison of CO_2, CH_4 and CO_2-equivalent (based on GWP_{20}) emission fluxes in different agro-ecosystems (e.g., aquaculture ponds, rice-fish farming systems, paddy fields and rice–wheat cropping systems). ND indicates no data. Numbers in parentheses are mean values.

Types	Location	Study period	CO_2 flux (mg C m^{-2} h^{-1})	CH_4 flux (mg m^{-2} h^{-1})	CO_2-eq flux (mg CO_2-eq m^{-2} h^{-1})	Reference
Aquaculture ponds	Min River Estuary, China	June–October 2015	-8.0 – 5.8 (1.3)	0.02 – 39.8 (4.7)	-22.3 – 4475.2 (528.4)	This study
	Jiulong River Estuary, China	June–October 2015	-2.7 –15.7 (4.2)	1.9 – 17.6 (7.2)	203.7 – 2035.0 (825.2)	Yang et al., 2018
	Zhangjiang River Estuary, China	January–December 2020	-84.2 –34.6 (-25.8)	0.02 – 2.8 (0.2)	— (-74.2)	Zhang et al., 2022
	Gaoqing, China	April–September 2013	13.8 – 41.2 (26.6)	ND	50.6 – 150.9 (97.7)	Chen et al., 2016
	Anhui Province, China	January–December 2016–2019	ND	0.4 – 60.1 (14.8)	33.6 – 5048.4 (1243.2)	Zhao et al., 2021
	Shanghai, China	July–September 2013	-9.6 – 100.4 (32.5)	0.5 – 36.2 (7.0)	32.4 – 3141.2 (620.5)	Zhu et al., 2016
	Jiangsu province, China	August 2017– August 2019	ND	0.8 – 1.0 (0.9)	67.2 – 84.0 (75.6)	Fang et al., 2021
	Northeastern, Brazil	ND	-42.9 – 5.6 (18.6)	-9.8 – 20.5 (5.3)	-1259.3 – 2309.7 (662.1)	Soares and Henry-Silva, 2019
	Suzhou, China	March 2013–March 2014	ND	6.8 – 10.7 (8.2)	757.7 – 1201.2 (923.2)	Yuan et al., 2021
	Ganyu County, China	ND	19.2 – 26.6 (5.5)	0.05 – 0.06 (ND)	75.5 – 103.5 (25.9)	Zhang et al., 2020
Rice-fish farming systems	Cuttack, India	July–December 2011	ND	0.7 – 10.6 (ND)	58.8 – 890.4 (ND)	Bhattacharyya et al., 2013
	ND	June to September 2003	ND	12.1 – 13.6 (12.9)	1016.4 – 1142.4 (1083.6)	Frei and Becker, 2005
	Cuttack, India	June–December 2005	ND	2.4 – 2.5 (2.5)	208.3 – 211.7 (210.0)	Datta et al., 2009
	Jiangjia village, northeast China	June–October 2013	ND	0.3 – 23.7 (11.9)	25.2 – 1990.8 (999.6)	Wang et al., 2019
Paddy fields	Xinghua, China	June 2014–June 2015	ND	0.6 – 0.7 (0.66)	50.4 – 58.8 (55.4)	Wu et al., 2018
	Yangtze River Delta, China	Rice seasons of 2005-2007	ND	-0.3 – 23.9 (ND)	-25.2 – 2007.6 (55.4)	Yao et al., 2012
	Taihu Lake region, China	June to October 2009 (2010)	ND	0.6 – 3.0 (1.8)	50.4 – 251.1 (147.2)	Hou et al., 2010
	Hunan province, China	Rice season in 2011 (2012)	ND	0.7 – 17.3 (ND)	58.8 – 1453.2 (ND)	Shen et al., 2014
	Chongqing, Southwest China	October 2009–October 2010	ND	0.9 – 3.0 (1.7)	75.6 – 252.0 (144.7)	Hao et al., 2016
Rice–wheat cropping systems	Taihu Lake District, China	January 2011 to November 2012	ND	-0.04 – 69.5 (ND)	3.4 – 5838.0 (ND)	Zhang et al., 2015
	Yangtze River Delta, China	June 2005 to June 2006	ND	-0.03– 57.0 (2.5)	2.5 – 4788.0 (211.6)	Yao et al., 2013
	Hubei Province, China	June 2012 to June 2018	ND	-0.8– 76.9 (4.1)	67.2 – 6459.6 (344.4)	Guo et al., 2021
	Jiangsu Province, China	June 2012 to May 2018	ND	-0.4– 1.0 (0.7)	33.6 – 84.0 (58.8)	Wu et al., 2019

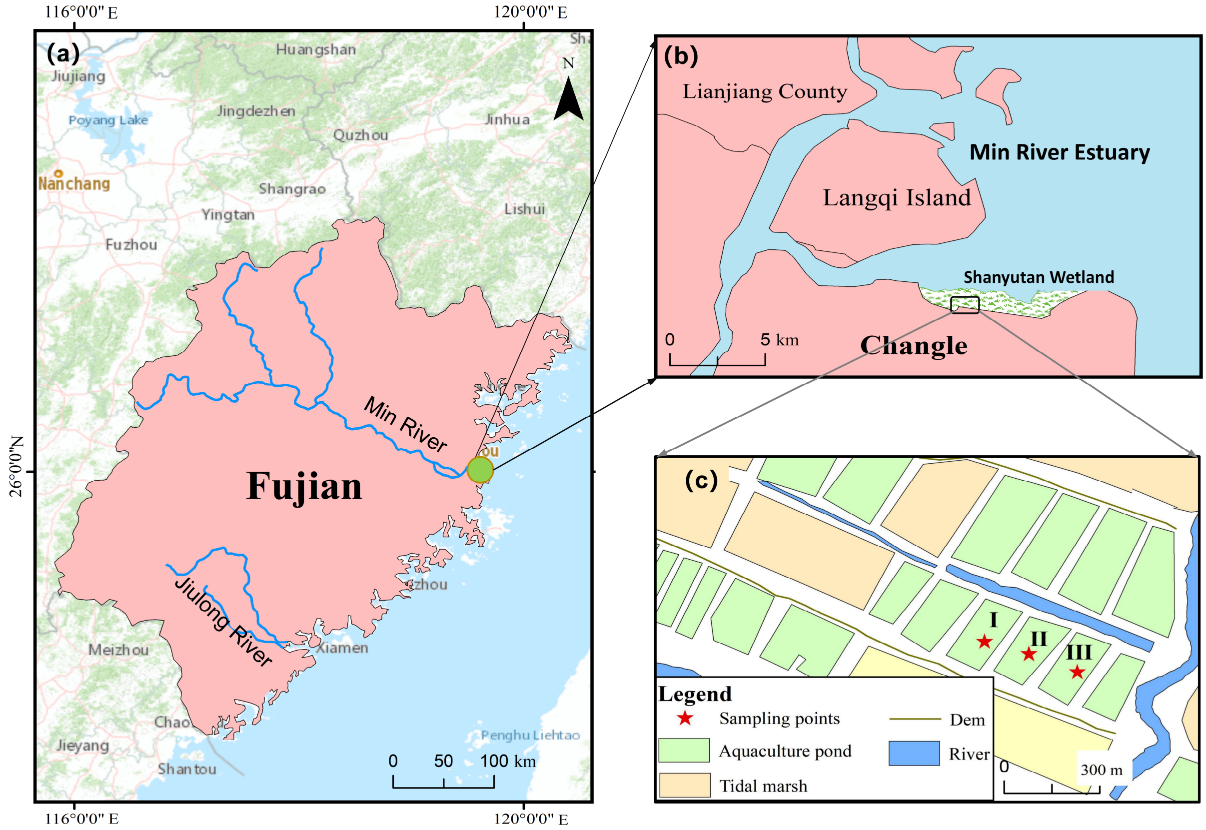

Figure 1. Location of the research areas (a, b) and sampling sites (c) within Shanyutan Wetland of the Min River Estuary (MRE) in Fujian, Southeast China.

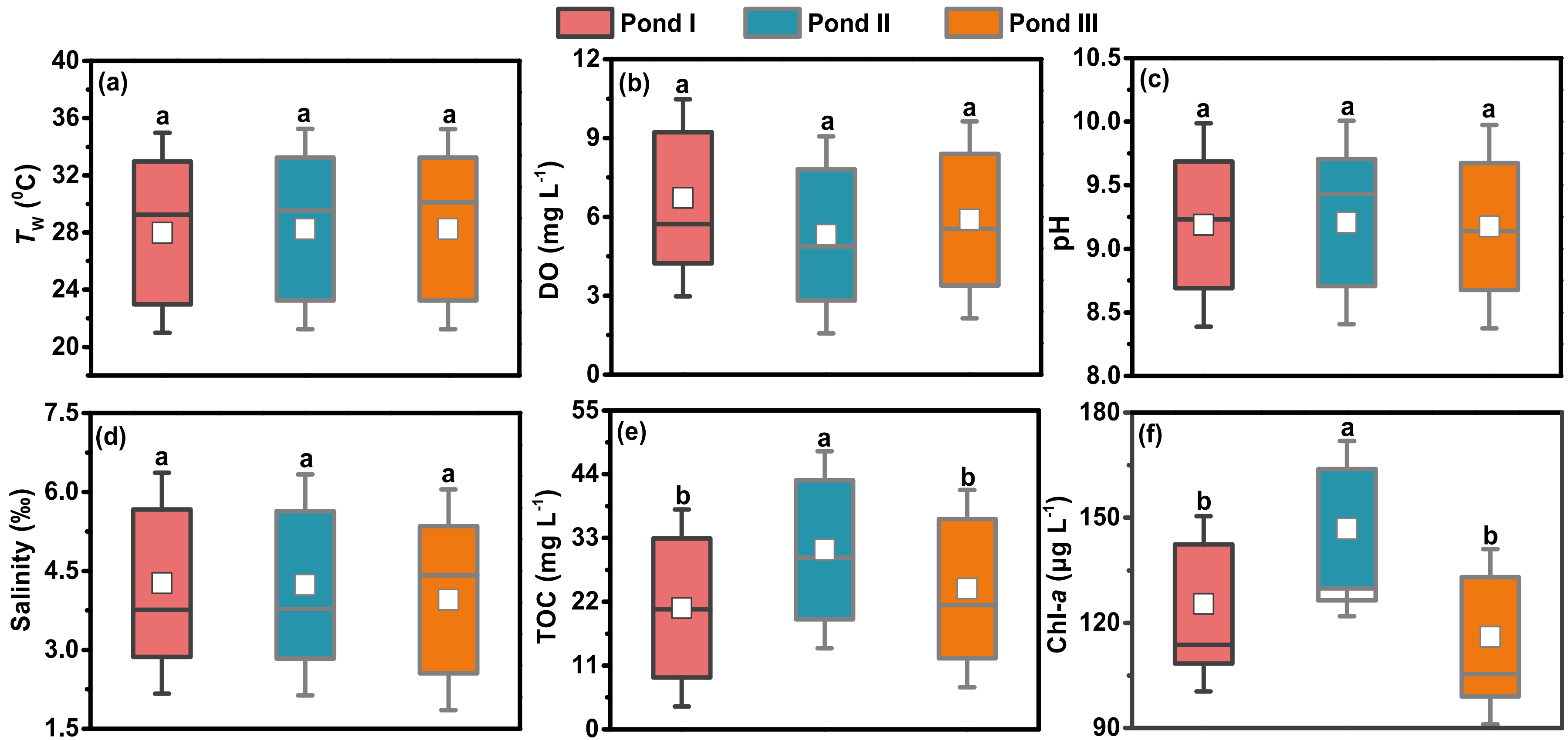

Figure 2. Boxplots of hydrographical parameters in the three shrimp aquaculture ponds (*Litopenaeus vannamei*) during the farming period. DO, T_W, Chl-*a* and TOC represent dissolved oxygen, water temperature, Chlorophyll *a*, and total organic carbon, respectively. Different lowercase letters above the bars show significant differences between sampling ponds ($n = 75$; $p<0.05$).

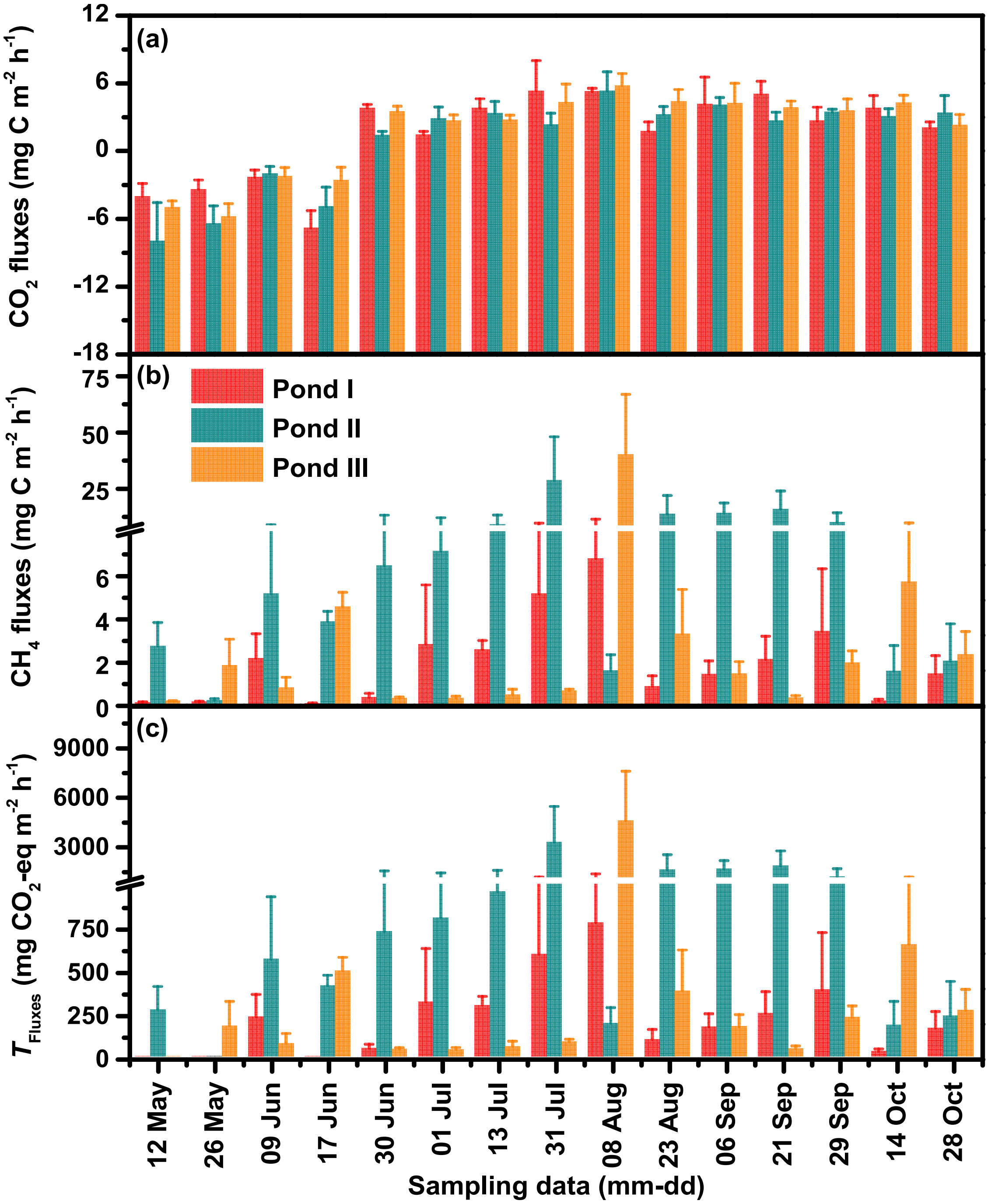

Figure 3. Temporal data of (a) CO_2 flux, (b) CH_4 flux, and (c) Total CO_2-eq flux (T_{Fluxes}) based on GWP_{20}, in the three shrimp aquaculture ponds (*Litopenaeus vannamei*) during the farming period (May to October). Error bars represent standard error (n = 5 sites).

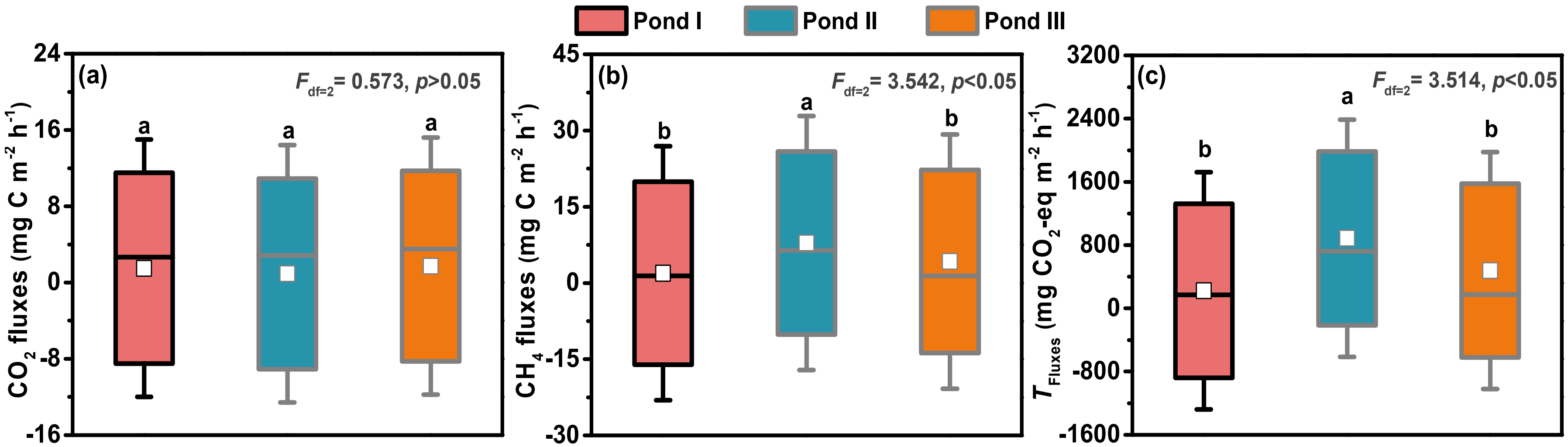

Figure 4. Variations in the (a) CO_2 flux, (b) CH_4 flux, and (c) Total CO_2-eq flux (T_{Fluxes}) based on GWP_{20}, in the three shrimp aquaculture ponds during the farming period (May to October). Different lowercase letters above the bars show significant differences between sampling ponds (n = 75; p<0.05).

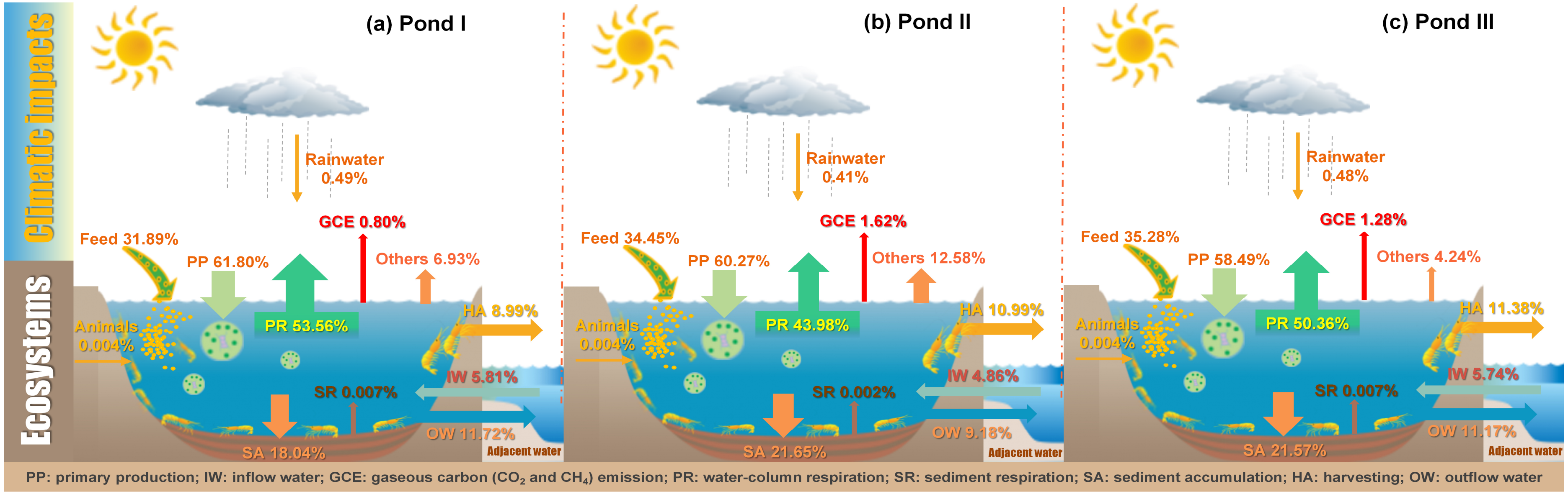

Figure 5. Percentages of carbon input and output components in the three shrimp aquaculture ponds (*Litopenaeus vannamei*) in the Min River Estuary during the farming period (May to October).

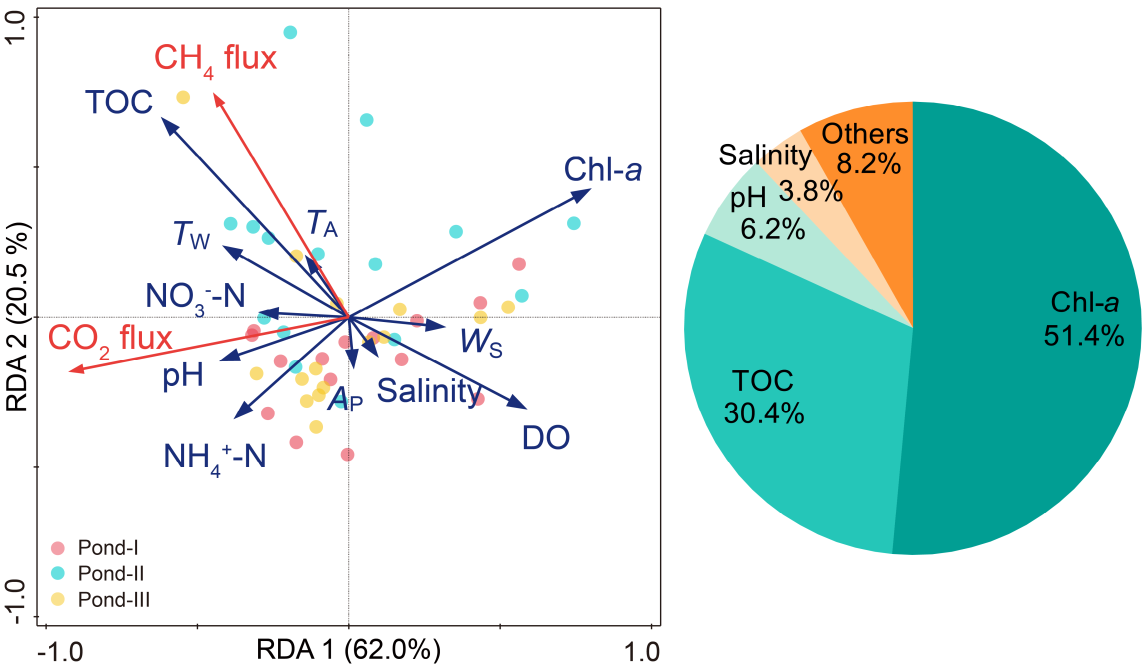

Figure 6. Redundancy analysis (RDA) biplots of the relationships between CO_2 and CH_4 fluxes and environmental variables (meteorological and hydrographical). The loadings of environmental factors (arrows) and the scores of observations in all sampling campaign are presented. A_P, T_A, W_S, T_W, TOC, DO, and Chl-*a* represent atmospheric pressure, air temperature, wind speed, water temperature, total organic carbon, dissolved oxygen, and chlorophyll *a*, respectively. The pie chart shows the explanatory power of the different environmental factors.